

Definitions and sharpness of the extratropical tropopause: A trace gas perspective

L. L. Pan and W. J. Randel

National Center for Atmospheric Research, Boulder, Colorado, USA

B. L. Gary and M. J. Mahoney

Jet Propulsion Laboratory, Pasadena, California, USA

E. J. Hints

Woods Hole Oceanographic Institution, Woods Hole, Massachusetts, USA

Received 3 May 2004; revised 13 September 2004; accepted 5 October 2004; published 4 December 2004.

[1] Definitions of the extratropical tropopause are examined from the perspective of chemical composition. Fine-scale measurements of temperature, ozone, carbon monoxide, and water vapor from approximately 70 aircraft flights, with ascending and descending tropopause crossings near 40°N and 65°N, are used in this analysis. Using the relationship of the stratospheric tracer O₃ and the tropospheric tracer CO, we address the issues of tropopause sharpness and where the transitions from troposphere to stratosphere occur in terms of the chemical composition. Tracer relationships indicate that mixing of stratospheric and tropospheric air masses occurs in the vicinity of the tropopause to form a transition layer. Statistically, this transition layer is centered on the thermal tropopause. Furthermore, we show that the transition is much sharper near 65°N (a region away from the subtropical jet) but spans a larger altitude range near 40°N (in the vicinity of the subtropical jet). This latter feature is consistent with enhanced stratosphere-troposphere exchange and mixing activity near the tropopause break. *INDEX TERMS*: 3334 Meteorology and Atmospheric Dynamics: Middle atmosphere dynamics (0341, 0342); 3362 Meteorology and Atmospheric Dynamics: Stratosphere/troposphere interactions; 0341 Atmospheric Composition and Structure: Middle atmosphere—constituent transport and chemistry (3334); *KEYWORDS*: tropopause definitions, stratosphere-tropopause exchange, tracer-tracer correlations

Citation: Pan, L. L., W. J. Randel, B. L. Gary, M. J. Mahoney, and E. J. Hints (2004), Definitions and sharpness of the extratropical tropopause: A trace gas perspective, *J. Geophys. Res.*, 109, D23103, doi:10.1029/2004JD004982.

1. Introduction

[2] Stratosphere-troposphere exchange (STE) in the extratropics is a key controlling factor for the ozone budget in the upper troposphere and water vapor variability in the lower stratosphere. With improved observational capability for both large and small scales, and with the advance in modeling tools in recent years, progress has been made in characterizing STE processes as well as quantifying their contributions [e.g., Wernli and Bourqui, 2002; Olsen *et al.*, 2002; Sprenger and Wernli, 2003; Stohl *et al.*, 2003; Cooper *et al.*, 2004]. Despite this progress, large uncertainties remain in quantifying the effect of STE on trace gas distributions in the upper troposphere (UT) and lower stratosphere (LS). In particular, the results of the model studies mentioned above, many of which are based on winds from large-scale meteorological data sets, are yet to be validated by independent observations. Chemical observations are particularly helpful in this respect.

[3] One of the difficulties of quantifying STE in the extratropics is the identification and characterization of the extratropical tropopause. Uncertainties in defining this boundary often make the quantitative study of STE an ill-posed problem. The tropopause has been defined using the temperature lapse rate (thermal tropopause) [*World Meteorological Organization (WMO)*, 1986], potential vorticity (PV) gradient or values (dynamical tropopause) [Danielsen, 1968; Shapiro, 1978; Holton *et al.*, 1995], and ozone gradient and values [Browell *et al.*, 1996; Bethan *et al.*, 1996]. In observational studies all three definitions are used under various conditions. Model investigations often use a PV based dynamical tropopause. A range of PV values from 1.5–3.5 PVU are used [Hoerling *et al.*, 1991; Holton *et al.*, 1995; Dethof *et al.*, 2000; Wernli and Bourqui, 2002]. It has been shown that these definitions agree qualitatively on the large scale, but can give different answers to the details of the tropopause location. The results of STE calculations may vary depending on what issues one wishes to address. In particular, the results of stratospheric contributions to upper tropospheric ozone may vary significantly depending on the tropopause definition used in the calculations.

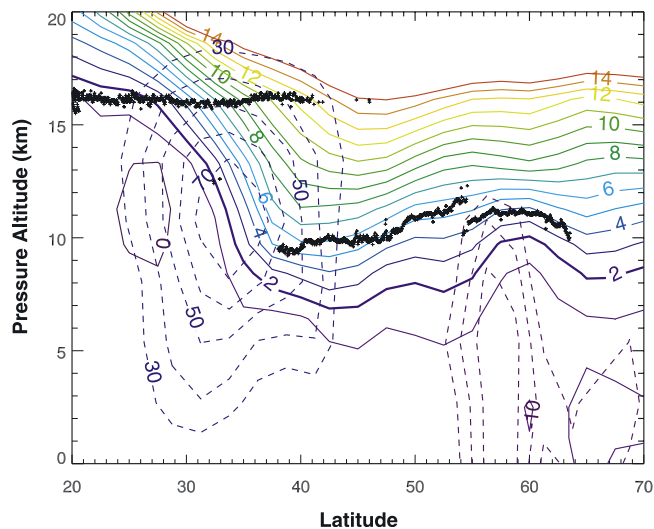


Figure 1. Comparisons of tropopause height given by thermal and dynamical definitions. The thermal tropopause heights (indicated by black crosses) are derived from MTP data, measured aboard the NASA DC-8 during TOTE/VOTE, 11 December 1995. The cross section is near 155°W longitude. The PV (solid contours) and zonal wind (dashed contours) fields are from Met Office data. The two colors used for the wind contours represent the westlies (blue) and easterlies (purple). Note the existence of double thermal tropopauses between 38°N and ~41°N.

[4] While the difference between the ozone profile based tropopause and the others have not been examined on the global scale, the difference between the thermal and dynamical definition is more evident in the vicinity of the subtropical jet (STJ). To illustrate the differences in the tropopause location given by the thermal and dynamical definitions, we show in Figure 1 a Northern Hemispheric cross section of the tropopause heights given by the two definitions. In Figure 1, the thermal tropopause height is measured by the Microwave Temperature Profiler (MTP) on board the NASA DC-8 research aircraft during the Tropical Ozone Transport Experiment/Vortex Ozone Transport Experiment (TOTE/VOTE). The PV and zonal winds are based on the Met Office analyses [Swinbank and O’Neill, 1994], interpolated to the flight cross section. Figure 1 illustrates that (1) the thermal tropopause and dynamical tropopause, if chosen as the 2 PVU surface, sometimes differ by more than 2 km; and (2) the difference of the two definitions is more significant in the vicinity of the STJ. As shown in Figure 1, the thermal tropopause is discontinuous in the vicinity of the STJ and can have two values simultaneously (a double tropopause produced by overlapping tropical and midlatitude air masses), whereas the dynamical tropopause is continuous.

[5] The difference between the two tropopause definitions is caused by the fundamental difference in the concepts behind the two definitions. The thermal definition is designed to locate the transition point in the thermal structure, vertically, between troposphere and stratosphere. The thermal definition therefore allows for multiple tropopause in a given location [e.g., Kochanski, 1955]. In the

vicinity of jets there is often a double tropopause (see Figure 1), each separating stratospheric and tropospheric air masses on either side of the jet. On the other hand, the dynamical tropopause is designed to locate a quasi-material surface that identifies the chemical transition from stratosphere to troposphere, as stated by Holton *et al.* [1995], “... the tropopause often behaves, chemically speaking, as if it were a material surface to a varying degree of approximation.” The PV based dynamical tropopause definition is established because PV is a conservative stratosphere tracer under conditions of adiabatic and frictionless flow [e.g., Hoskins, 1991].

[6] The primary motivation of this paper is to examine, using observations, how well the thermal and dynamical tropopauses identify the chemical transition from troposphere to stratosphere. Using fine-scale observations of chemical tracers, we look for answers to a set of questions: What is a more meaningful definition of the extratropical tropopause when investigating STE of chemical tracers? Is the extratropical tropopause better characterized as a surface or a layer? How do we best define or locate this surface or layer? We argue that a meaningful definition should be consistent with the change of chemical composition across the tropopause region.

[7] Our study is closely related to a group of observational studies that examined mixing in the vicinity of the tropopause using tracer relationships [Fischer *et al.*, 2000; Hoor *et al.*, 2002; Zahn *et al.*, 2000, 2004]. In particular, using the O₃-CO relationship in the midlatitude tropopause region, Fischer *et al.* [2000] and Hoor *et al.* [2002] have concluded that a mixing layer is formed in the lowermost stratosphere right above the tropopause, as a result of troposphere to stratosphere transport. This mixing layer has later been referred to as the transition layer between troposphere and stratosphere [WMO, 2003]. We present in this paper a statistical analysis, using tracer relationships and simultaneously measured temperature profiles, to show that this mixing layer is indeed a transition layer between the stratosphere and troposphere. We further show that the chemical transition is centered on the thermal tropopause and that it is more appropriate to interpret the transition layer as the result of two-way STE, rather than one-way troposphere to stratosphere transport.

[8] The O₃-CO relationship has also been used as a new way of defining a chemical tropopause [Zahn *et al.*, 2004]. An additional motivation for this work is to further examine the definition of the chemical tropopause, and its relationship with the transition layer.

2. Description of Data

[9] In Figure 1, the thermal tropopause is derived from the measurements of the MTP. MTP is a passive microwave radiometer that measures the natural thermal emission from oxygen molecules at three frequencies (55.51, 56.66 and 58.79 GHz) [Denning *et al.*, 1989]. The vertical resolution of an MTP profile is ~0.2 km within 2 km of the flight altitude, and decreases with distance from the flight altitude so that for altitude differences of 10 km the resolution is ~2km. For the nominal DC-8 cruising altitudes of 10 to 12.5 km, the MTP exhibits a postmission validated accuracy of <1.0 K throughout the altitude region 8.5 to 16.5 km,

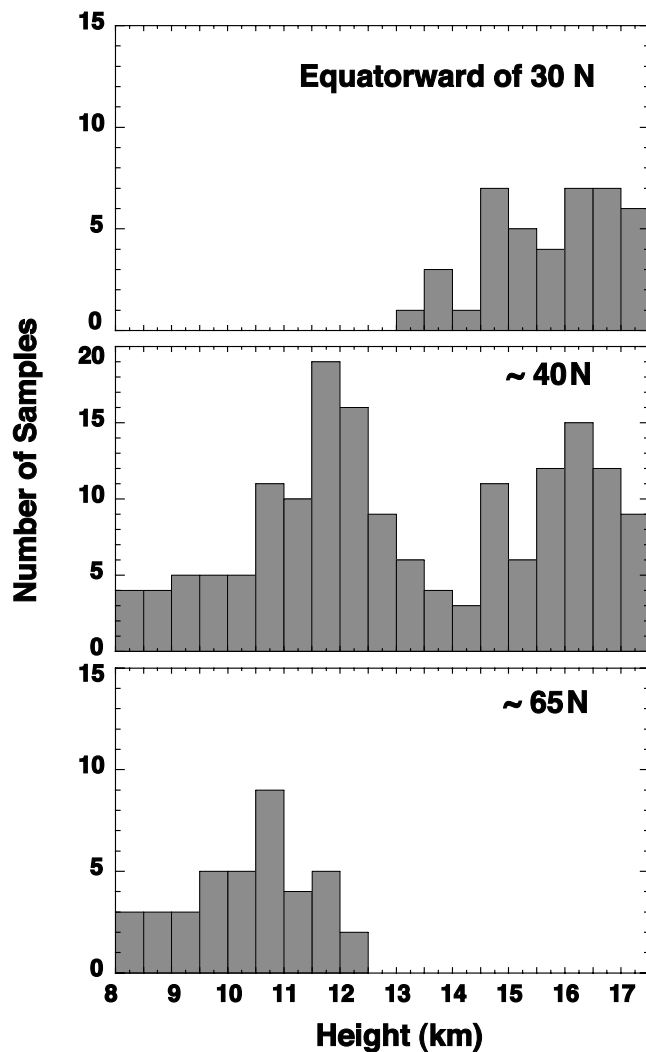


Figure 2. Histogram of the tropopause height sampled by ER-2 during STRAT and POLARIS.

<2.0 K from 5 to 21 km, and <3.0 K from 4 to 26 km. Typical uncertainties in thermal tropopause heights range from 0.2 km when the aircraft is near the tropopause to 0.5 km when the aircraft is 5 km away.

[10] The statistical study presented in this paper uses in situ measurements on board the NASA high-altitude ER-2 research aircraft during the Stratospheric Tracers of Atmospheric Transport (STRAT) and Photochemistry of Ozone Loss in the Arctic Region In Summer (POLARIS) campaigns. The two missions were carried out during 1995–1997. The STRAT campaign focused on the measurement of long-lived tracers and dynamical quantities as functions of altitude, latitude, and season in order to help determine rates for global-scale transport. The objective of POLARIS was to understand the behavior of polar stratospheric ozone as it changes from high concentrations in spring to low concentrations in autumn.

[11] In situ CO measurements during STRAT and POLARIS were made by the Aircraft Laser Infrared Absorption Spectrometer (ALIAS) [Herman *et al.*, 1999]. The measurement accuracy for CO is better than 10%. The O₃ data are from NOAA ultraviolet absorption spectroscopy

instrument [Proffitt and McLaughlin, 1983]. In situ water vapor data used in this analysis are from the Harvard Lyman- α hygrometer [Weinstock *et al.*, 1994], which have been shown to have an accuracy of $\pm 5\%$ [Hirta *et al.*, 1999]. Coincident temperature and pressure data on the ER-2 were obtained by the Meteorological Measurement System (MMS) [Scott *et al.*, 1990], with accuracies of <1 K and 0.3 mb, respectively. Tropopause heights were determined for the ER-2 flights from combinations of MMS in situ air temperature and MTP remotely sensed temperature profiles, using the standard WMO definition for the thermal tropopause.

3. Transition of Troposphere and Stratosphere Characterized by Static Stability and the Tracer Profiles

[12] The ER-2 during STRAT and POLARIS made ~ 140 tropopause crossings during the ascending and descending segments of 71 flights. These crossings occurred in the vicinity of three locations: Barbers Point, Hawaii ($\sim 21^\circ\text{N}$), Moffett Field, California ($\sim 37^\circ\text{N}$), and Fairbanks, Alaska ($\sim 65^\circ\text{N}$). The measurements near California were made between 1995 and 1997, and sampled all seasons. The measurements near Alaska were made during 1997 and sampled Spring to Fall (April to September, but without August). Figure 2 shows the distribution of the thermal tropopause height for all flights. As expected, Figure 2 shows a higher tropical tropopause equatorward of 30°N , a transition from the higher tropical tropopause to the lower midlatitude tropopause in the vicinity of 40°N , and an even lower tropopause near 65°N . Because of the influence of the STJ, the distribution of the thermal tropopause height is bimodal in the vicinity of 40°N . One component is higher than 14 km with the peak of the distribution around 16 km, and the other is below 14 km with its peak around 12 km. This supports that the thermal tropopause break in the subtropics, shown by the example in Figure 1, is not an isolated occurrence but a statistically persistent feature. Although not a new finding, this is highly relevant to the trace gas analysis we present later in the paper, because it shows that, because of the latitudinal meandering of the STJ, the measurements near 40°N sampled either the tropical or the extratropical air depending on the position of the STJ.

[13] To demonstrate that we have selected the thermal tropopause correctly, we first examine the change in thermal structure across the thermal tropopause. Since the thermal definition is designed to separate the troposphere from the stratosphere according to the air mass's static stability, we show in Figure 3 vertical profiles of static stability, represented by the buoyancy frequency squared, in the coordinates of height relative to the WMO tropopause. We have divided the data near 40°N into two groups and consider the group with tropopause heights above 14 km to be characteristic of tropical air, while the group below 14 km is characteristic of extratropical air. An abrupt change in the thermal structure at the tropopause is very pronounced for the mid and high-latitude tropopause (Figure 3, middle and bottom), but it is less pronounced for the tropical tropopause (Figure 3, top). Figure 3 demonstrates that we have successfully applied the WMO definition and that the thermal

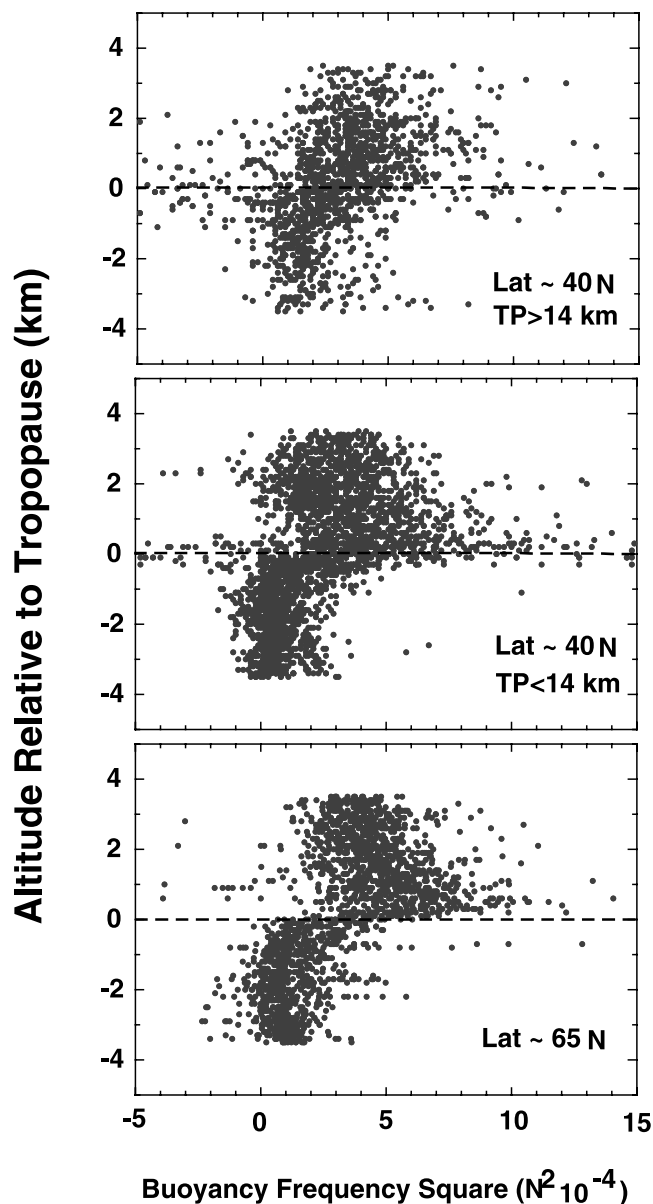


Figure 3. Static stability (N^2) as a function of altitude relative to the thermal tropopause. This figure demonstrates that the thermal tropopause successfully locates the sharp discontinuity in static stability for both 65°N and 40°N locations. It further shows that the transition in thermal structure is more gradual for the upper (tropical) tropopause near 40°N .

tropopause marks the sharp discontinuity in the thermal structure in the extratropics.

[14] Although it is not the focus of this paper, it is worth noting that the sharp discontinuity across the thermal tropopause, from N^2 values of $\sim 1 \times 10^{-4}$ in the upper troposphere to $\sim 5 \times 10^{-4}$ immediately above the tropopause, is very similar to the results of *Birner et al.* [2002], who used a high-resolution radiosonde based climatology from two midlatitude locations (48°N and 49°N) to show that there is a maximum of $N^2 \sim 6 \times 10^{-4}$ immediately above the tropopause. The stability maximum is associated

with a sharp temperature inversion above the tropopause. Our results indicate that the inversion discussed by *Birner et al.* [2002] occurs not only at high-latitude locations but also at subtropical locations.

[15] We are interested in determining whether tracers also exhibit a sharp discontinuity at the thermal tropopause. Figure 4 presents the vertical profiles of CO (a tropospheric tracer) and O_3 (a stratospheric tracer), measured near 65°N , as function of height (top), potential vorticity (middle), and relative height with respect to the thermal tropopause (bottom). PV is obtained from a large-scale NASA Goddard model and was generated as part of mission support. Figure 4 shows the contrast of the air mass's variability when grouped by different criteria: The tracers as function of altitude (top) show the natural variability of tracer profiles in altitude coordinates. A comparison of Figure 4 (bottom) with Figure 4 (top and middle) shows that the data become much more compact when plotted as a function of height relative to the thermal tropopause. This indicates that the thermal tropopause not only marks the sharp change in the thermal structure, but also identifies the discontinuity in chemical composition.

[16] We next examine whether the sharpness of the transition varies with latitude. Figure 5 shows profiles of carbon monoxide, ozone, and water vapor as functions of altitude relative to the thermal tropopause height for both 40°N and 65°N locations. All three tracers show an organized change when plotted with respect to height relative to the thermal tropopause. There is, however, a marked difference between the two latitudes, with the 40°N group showing a less abrupt change at the tropopause. Note that there are some sampling differences between the measurements at these two latitudinal locations. There are more samples in the 40°N location and all seasons are covered. The 65°N location was sampled by fewer flights and only during April to September. We have examined and confirmed that the characteristics of 40°N profiles do not change if the measurements during late fall and winter months are removed. Also note that there are two groups of thermal tropopauses in the 40°N region (as shown in Figure 2), and the thermal transition of the two groups are different (as shown in Figure 3). To isolate the potential cause of the less abrupt change in the tracer profiles near 40°N , we show only the tracer profiles across the lower tropopause (height < 14 km) in Figure 5. The differences between the 40°N and 65°N groups may be due to more frequent STE activities in the vicinity of the tropopause break. The transition and the latitudinal variation are further examined in terms of tracer relationships in the following section.

4. Transition Between Stratosphere and Troposphere Characterized by Tracer Relationships

[17] As discussed in the introduction, tracer relationships from airborne measurements, the O_3 -CO relationship in particular, have been used [*Fischer et al.*, 2000; *Hoor et al.*, 2002; *Zahn et al.*, 2000] to infer STE. In particular, using measurements from the STREAM campaign, *Fischer et al.* [2000] and *Hoor et al.* [2002] identified a mixing layer above the local tropopause. Using CARIBIC campaign

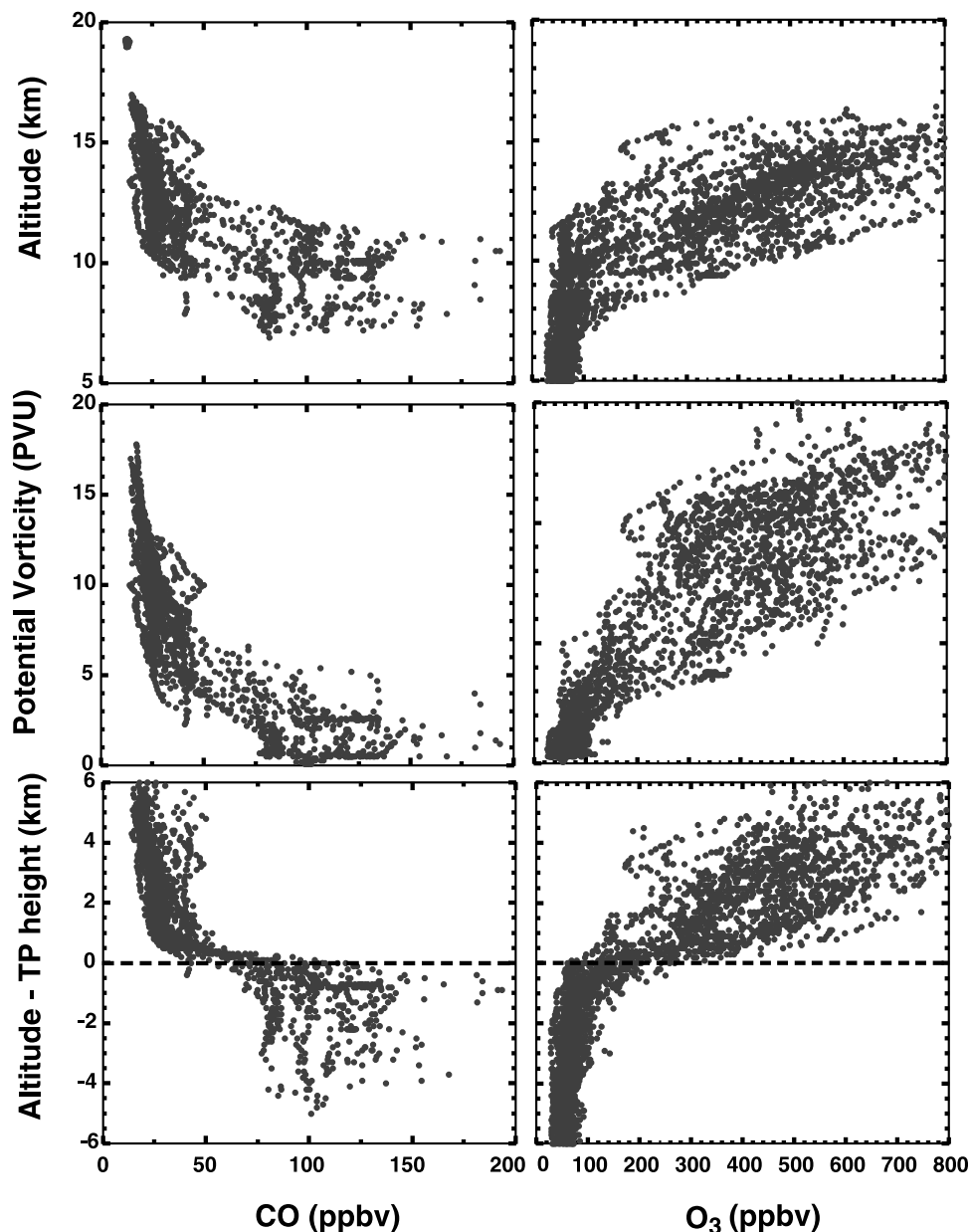


Figure 4. CO and O₃ profiles near 65°N as functions of altitude, potential vorticity, and relative altitude with respect to the thermal tropopause.

data, Zahn *et al.* [2004] has proposed using the O₃-CO relationship to identify the location of the chemical tropopause. The analysis presented here provides new information and different perspectives with two main advantages. First, the ER-2 data used in this work cover a much greater altitude range (approximately 5–20 km in altitude, compared to 9–12 km in CARIBIC [Zahn *et al.*, 2000, 2004] and 8–12.5 km in STREAM [Hoor *et al.*, 2002]). This greater ER-2 coverage allows a clear characterization to be made of the stratosphere, the troposphere and the transition region in tracer space. Second, the vertical crossings of the tropopause region during ascents and descents with collocated temperature measurements allow an accurate identification of the thermal tropopause and as well as an examination of the change in tracer relationships with respect to the change in the thermal structure.

[18] Building upon these recent analyses [Fischer *et al.*, 2000; Hoor *et al.*, 2002], we explore the use of tracer relationships in the upper troposphere and lower stratosphere (UTLS) as a way of characterizing the transition between stratosphere and troposphere. Figure 6 is a schematic that illustrates the connection between tracer profiles in altitude space and tracer-tracer space in the UTLS region. As indicated in Figure 6, if we have a tracer of stratospheric origin (e.g., ozone) and a tracer of tropospheric origin (e.g., CO or H₂O), while tracer profiles across the tropopause show a decrease away from the source region, the tracer relationship form an “L” in tracer-tracer space. The stratospheric air parcels form the upper branch of “L”, because there is a rapid increase of stratospheric tracer accompanied by a small value and small variability of the tropospheric tracer in the stratosphere. Similarly, the tropospheric air

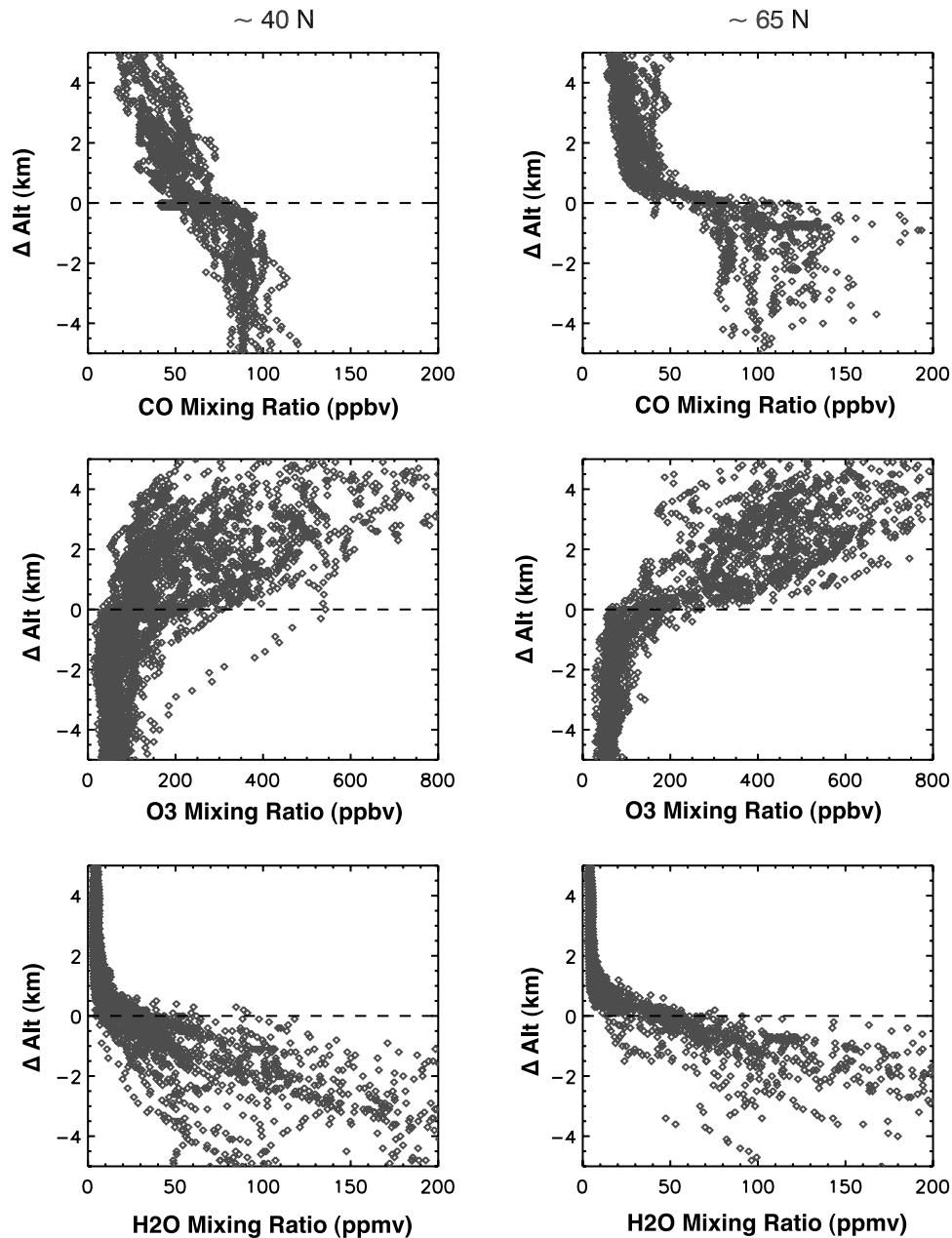


Figure 5. Trace gas profiles as a function of altitude relative to the thermal tropopause height in two extratropical locations. For the 40°N location, only the lower tropopause (tropopause height <14 km) profiles are included here.

parcels form the lower branch of the “L”. We suggest that the transition point between the two branches should be considered as the chemical tropopause. The nature of the connection between the two branches provides information on the characteristics of the transition, that is, the sharpness of the tropopause.

[19] To illustrate the concept represented in the schematic, we have selected a specific case using data from a POLARIS flight on 10 July 1997 (970710). This was a “stacked flight” (consisting of flight at many altitudes at the same location) designed to study the upper troposphere. Both ascending and descending portions of the measurements are shown in Figure 7. The thermal tropopause height, marked by the dash lines, was 10.8 km for both

ascending and descending profiles. Figure 7a displays temperature and PV profiles. Figure 7b displays CO and O₃ profiles. Figure 7c shows the O₃-CO correlation in this case, with the data points above the thermal tropopause in red and below in green. As shown in Figure 7, the temperature profile supports our identification of the tropopause height. Both tracer profiles go through a rapid change across the thermal tropopause, indicating the thermal tropopause in this case marks the chemical boundary between the stratosphere and troposphere. This is further supported by the O₃-CO correlation, where the two branches of the “L” shape are formed by a strong negative correlation in the stratosphere and a small positive correlation in the troposphere. The positive correlation is due to the fact that the

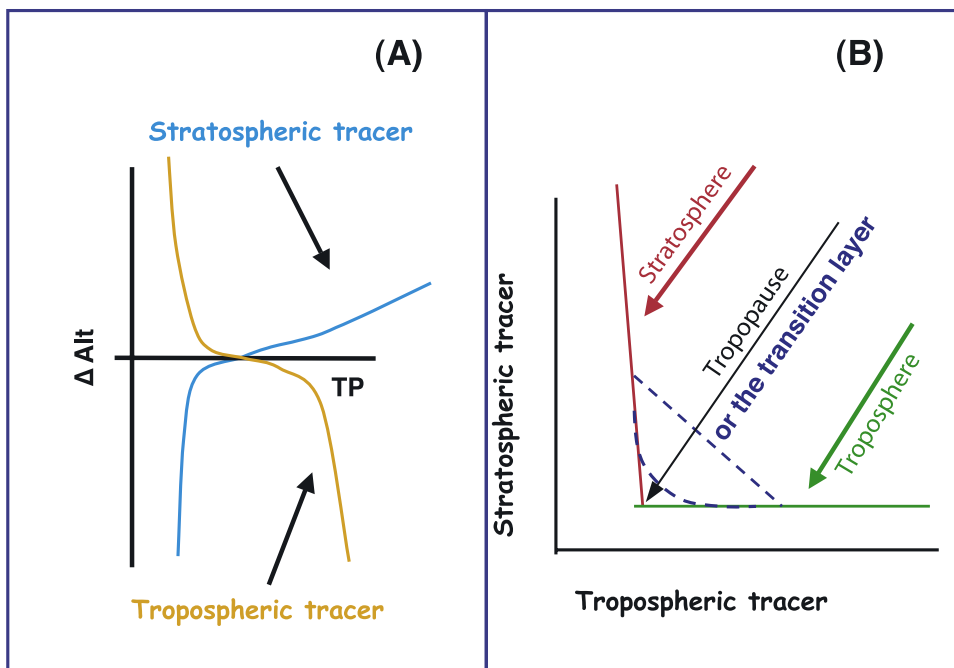


Figure 6. Schematic illustrating the concept of identifying the tropopause location using tracer relationships: (a) stratospheric tracer and a tropospheric tracer in altitude space and (b) their relations in tracer-tracer space.

two trace gases share common sources in the troposphere and are chemically related [Fishman and Seiler, 1983]. Figure 7 also shows that the “corner” of the “L” is cut off by “mixing lines”, formed by air parcels with a mixture of stratospheric and tropospheric composition. In this case, the mixing lines are well approximated by a straight line. The mixing lines have a stratospheric end point with ~380 ppbv for ozone and ~30 ppbv for CO, and a tropospheric end point with 50–100 ppbv for ozone and ~100 ppbv for CO. If we decide to choose a “chemopause” on the basis of the tracer relationships, we could choose the midpoint of the mixing line, which is very

close to the thermal tropopause (transition of red and green). This is consistent with Figure 7b, indicating the thermal tropopause in this case also marks the chemical transition. Using 2 PVU as the tropopause in this case would have placed the tropopause about 1 km lower. Similarly, using the O₃ profile alone to define the tropopause would likely locate a tropopause ~1 km below the thermal tropopause (similar to that observed by Browell *et al.* [1996] and Bethan *et al.* [1996], which are ~ 500–800 m below the thermal tropopause), and using the CO profile alone (approaching from the stratospheric side) would likely to identify a tropopause ~1 km above the thermal

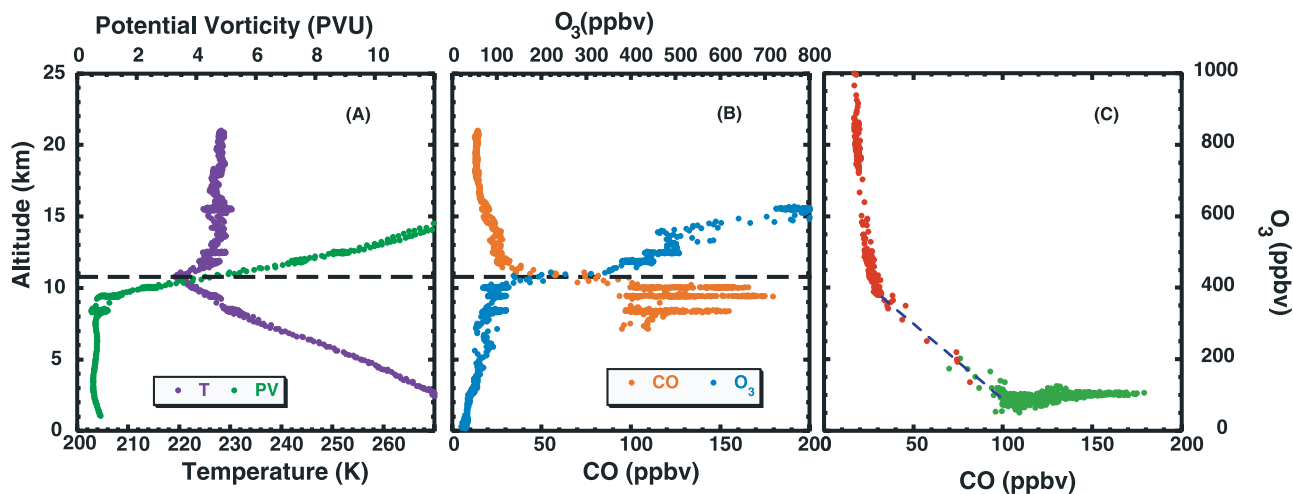


Figure 7. Profiles from POLARIS flight 970710 near Fairbanks. Data from both ascending and descending portions of the flight are shown. The thermal tropopause, represented by dashed lines, is at 10.8 km.

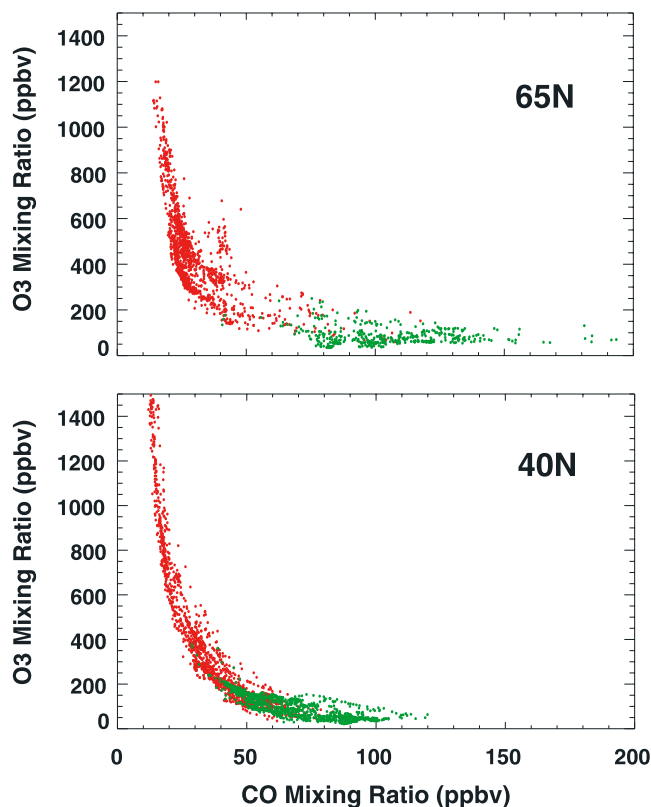


Figure 8. Relationship of stratospheric tracer O_3 and tropospheric tracer CO for the two extratropical locations sampled by ER-2 during STRAT and POLARIS. Measurements below the thermal tropopause are green and measurements above are red.

tropopause. This example demonstrates that the “chemical tropopause” is not equivalent to the “ozone tropopause”, and a better way of defining the “chemopause” is to use stratosphere-troposphere tracer relationships. When the tracers are examined together, it becomes evident that the chemical transition has a finite depth of 1–2 km.

[20] We next examine the transition statistically. Figure 8 shows the O_3 -CO relationship for all STRAT and POLARIS flights near the two extratropical locations. Similar to the schematic and the example, CO and O_3 in the UTLS form “L”-shaped relationships. The relationships are fairly compact. The upper branch, formed by stratospheric air parcels, is marked by large ozone mixing ratios (typically greater than 300 ppbv) and small CO mixing ratios (typically less than 30 ppbv), and it is also marked by a strong negative correlation of the two tracers. The lower branch of the “L”, formed by tropospheric air parcels, is marked by an enhanced CO (50–200 ppbv) and low O_3 (less than 100 ppbv). In the case of 65°N, the lower branch exhibits positive correlation (shown more clearly in Figure 9), indicating that the air parcels are largely of tropospheric origins, but the 40°N group has a negative O_3 -CO correlation, indicating enhanced influence of stratospheric air.

[21] It is evident from Figure 8 that the transitions between the stratospheric and tropospheric branches do not form a sharp “corner” in general. The modification of the corner by a gradual transition indicates the existence of a

transition layer. A detailed examination of data show that the transition layer in tracer-tracer space consists of many mixing lines, formed by air parcels of different ratios of stratospheric and tropospheric air. The lengths of the mixing lines appear to be characteristically different for the two locations. The mixing lines at 65°N are more distinct and can be approximated by straight lines, which indicate that the mixing activity is between distinct air masses that are separated by long range in tracer space. This is consistent with the indications given by Figures 5 and 7, where the 65°N tracer profiles exhibit abrupt change across the tropopause. The mixing lines in the 40°N region, on the other hand, are less distinct. Closer examination reveals that they are generally much shorter. The transition region, in tracer-tracer space, therefore appears to be curved and more compact. This is an indication that the mixing in this region is more vigorous so that the mixing is continuous and between similar air masses, or air masses closer in tracer space. This is also consistent with Figure 5, where the 40°N profiles show a gradual change across the tropopause. Physically, these two situations are very similar to what have been discussed by *Plumb et al.* [2000] for the mixing in the vicinity of the polar vortex, where both types of mixing are discussed on the basis of observations.

[22] To further examine the location and the spatial distribution of the transition layer, we use a set of rules to select the points that belong to the transition layer. The range and distribution of this layer can then be characterized. The strategy is to first establish empirical O_3 -CO relationships for the stratosphere and troposphere in the tracer space. Those data that are outside of both relationships will then be considered to be part of the transition layer. Specifically, the stratospheric relationship is established by a polynomial fit to all data with CO mixing ratio less than 25 ppbv. The tropospheric relationship is established by a linear fit to all points with O_3 less than 70 ppbv. The resulting regression lines and the range of 3σ (where σ is the standard deviation of the residuals) are shown in Figure 9. The transition layer, that is, the data points outside the 3σ boundaries of both stratospheric and tropospheric relationships, is identified in the tracer space and shown as blue points in Figure 9. The distribution of the transition points in altitude space can then be calculated and plotted relative to the altitude of the thermal tropopause, as shown in Figure 9 (middle). Similarly, the distributions of transition points in PV are given in Figure 9 (bottom).

[23] Figure 9 confirms the observations of Figures 7 and 8 that the transition layer, as defined above, is centered on the thermal tropopause with a sharp peak in the distribution for both locations. At 65°N the transition layer spans ~2–3 km and exhibits a slightly higher population above the tropopause. One possible source for the skewed distribution is identified as the group of data circled (by the black oval). These data appear to depart from the compact relationship. Preliminary investigation shows that these points are measured in the 350 to 370 K potential temperature range, several kilometers above the local tropopause, and represent an air mass very different from the local environment. They are likely to originate from a deep intrusion event due to Rossby wave breaking, similar to that discussed by *O’Connor et al.* [1999] and *Bradshaw et al.* [2002]. An additional factor that could contribute to the apparent bias

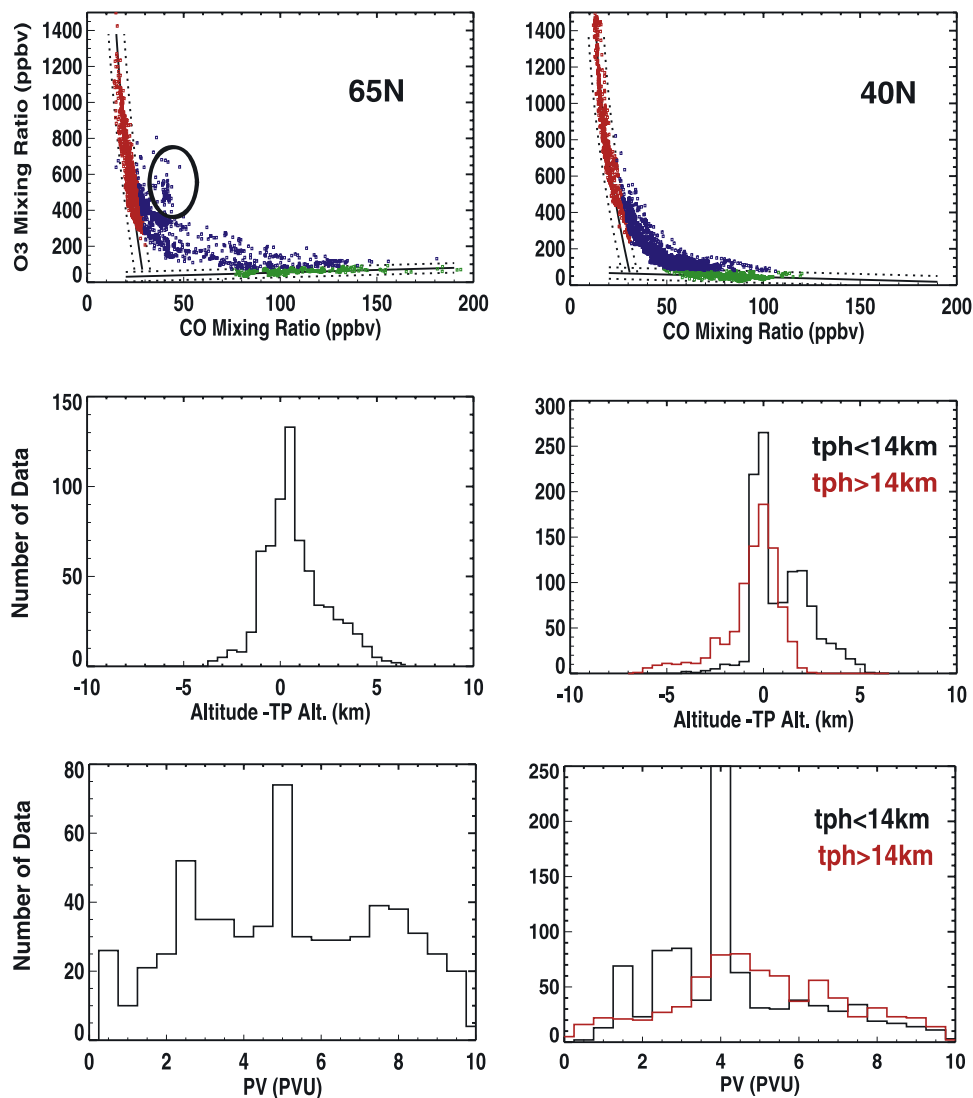


Figure 9. Location and thickness of the transition layer. (top) Same data as in Figure 8, with solid lines representing the empirical stratospheric and tropospheric O₃-CO relationships, derived using data points with CO < 25 ppbv for stratospheric and O₃ < 70 ppbv for tropospheric. The points outside 3σ (marked by the dotted lines) of both relationships are considered transition points. The stratospheric, tropospheric, and transitional points are represented by red, green, and blue, respectively. (middle) Altitude distribution of transition points (blue) relative to the thermal tropopause. In the case of 40°N the distributions are given as two populations, depending on whether the respective thermal tropopause height is below or above 14 km. (bottom) PV distribution of the transition points. The 40°N distributions are given as two populations.

toward above-tropopause altitudes is that there is an enhanced troposphere to stratosphere exchange for the sampled time period (note again that the 65°N region are sampled during April to September).

[24] For the measurements at 40°N, we have presented the distribution as two populations depending on the height of the thermal tropopause with which each measurement is associated. The distribution for the lower layer is skewed toward higher altitudes, with a possible secondary peak around 3 km above the local thermal tropopause. The distribution of the upper layer is skewed toward lower altitudes. This indicates that the active mixing in the region of the STJ occurs mostly through the tropopause break, that is, above the lower (extratropical) tropopause and below the

upper (tropical) tropopause. Note that the centers of these two groups are separated ~ 4 km in altitude, statistically, as shown in Figure 2. As a result, the transition layer in the vicinity of the STJ spans a wider range of altitude and is approximately 6 km (the blue points in Figure 9 (top right) cover from 10 to 16 km in altitude).

[25] Figure 9 (bottom) show that distributions of transition layer as a function of PV span a broad range of PV values (roughly 1–10 PVU). This can be attributed to two factors. One is that PV is calculated from large-scale meteorological data and may not resolve features at the small scales captured by the observed chemical tracers. The other is that the transition from the troposphere to the stratosphere may be better characterized by the isentropic

gradient of PV, rather than a specific constant value of PV. Figure 1 is an example of how the transition can occur at different PV values.

5. Conclusions and Discussions

[26] We have examined trace gas profiles and tracer-tracer relationships in the extratropical UTLS region using high-resolution in situ measurements. Analyses of how the chemical transition is related to the thermal transition are given both statistically and with a selected profile. These analyses are motivated by the need to better characterize the extratropical tropopause, which should lead to improvement of quantitative investigation of the STE of chemical tracers, such as ozone and water vapor.

[27] On the basis of the trace gas analyses presented, we conclude that in the extratropics the chemical transition occurs in the vicinity of the thermal tropopause. Our results show that mixing of stratospheric and tropospheric air masses in the vicinity of the tropopause form a transition layer, indicating the effect of two-way exchange between stratosphere and troposphere. This layer has been previously observed [Fischer *et al.*, 2000; Hoor *et al.*, 2002], but considered a mixing layer, located above the local tropopause (when 2 PVU is used as the tropopause) as a result of troposphere to stratosphere transport. Our analyses provide a better characterization of this transition layer, largely because of the much greater altitude coverage in data and the inclusion of collocated temperature profiles. This conclusion is consistent with the results of Logan [1999], where the ozonesonde data were used to show that the seasonal cycle of UTLS ozone changes from the June–July maximum below the thermal tropopause to the March maximum above the thermal tropopause, indicating that the thermal tropopause characterizes the transition between the upper troposphere to the lower stratosphere in chemical composition.

[28] The existence of this transition layer argues that, in regards to chemical composition, the extratropical tropopause should be characterized as a layer, not a surface. The center of this transition layer is statistically associated with the thermal tropopause. The thickness of this layer varies with latitude. It appears to be ~ 2 – 3 km for locations away from the STJ region, however, it expands into a thicker layer in the vicinity of the STJ due to enhanced mixing activity near tropopause break. More extensive measurements are required to characterize the seasonal variability of the transition layer.

[29] Our analyses show that tracer-tracer relationships are a powerful tool for characterizing the extratropical UTLS region. It has significant advantages over using a single tracer, such as ozone, in locating the tropopause. We show that the “chemical tropopause” is not equivalent to the “ozone tropopause”, and a better way of defining the “chemopause” is to use stratosphere-troposphere tracer relationships. Figure 7 gives a good example. Although this approach is similar to that of Zahn *et al.* [2004], our analysis is different in that we rely upon a statistical characterization of the transition layer instead of attempting to identify the tropopause as a single point. Our results therefore provide new perspectives on the transition from stratosphere to troposphere. One of the new perspectives is

that air with ~ 100 ppbv of ozone, commonly considered to be stratospheric air, is more likely to be at the bottom of this transition layer.

[30] In addition to these conclusions, our analyses raise several issues in using PV to define the tropopause, especially when interpreting in situ measurements. While the transition layer identified by tracer relationships coincides with the thermal tropopause, it spans a broad range of PV values. This reflects two contributing factors. The first is that the dynamical tropopause definition, fundamentally, was not based on specific values of PV, but on the discontinuity in the PV field on isentropic surfaces [Danielsen, 1968]. It is very likely that the PV values that mark the air mass transition from troposphere to stratosphere vary with latitude and season. The second is that PV is not a measurable quantity at the scale of in situ measurements [Hartmann *et al.*, 1989]. Although it often works well as a stratospheric tracer in model studies, our results show that it can lead to misinterpretation of experimental data if not used carefully. In addition, it needs to be recognized that like chemical tracers, PV is not perfectly conserved. That is, conditions under which it is conserved (adiabatic, frictionless flow) are not always good assumptions in the tropopause region. Under what conditions and timescales these are good assumptions in the UTLS region warrants future investigation.

[31] Finally, the conclusions we have drawn are based on limited observations. We hope that the new generations of satellite data, those from the AURA satellite in particular (since the instruments are designed to have high vertical resolution data in the UTLS region), will provide global perspectives on these issues. Future airborne observations focused on the tropopause region are also needed to help better characterize the mechanisms of chemical mixing in the transition layer.

[32] **Acknowledgments.** This work is supported in part by the National Science Foundation through its support to the University Corporation for Atmospheric Research, by the NASA Upper Atmosphere Research Satellite guest investigator program, and by the NASA Atmospheric Chemistry Modeling and Analysis Program. Work performed at the Jet Propulsion Laboratory, California Institute of Technology, was carried out under a contract with the National Aeronautics and Space Administration.

References

- Bethan, S., G. Vaughan, and S. J. Reid (1996), A comparison of ozone and thermal tropopause heights and the impact of tropopause definition on quantifying the ozone content of the troposphere, *Q. J. R. Meteorol. Soc.*, *122*, 929–944.
- Birner, T., A. Dörnbrack, and U. Schumann (2002), How sharp is the tropopause at midlatitudes?, *Geophys. Res. Lett.*, *29*(14), 1700, doi:10.1029/2002GL015142.
- Bradshaw, N. G., G. Vaughan, and G. Ancellet (2002), Generation of layering in the lower stratosphere by a breaking Rossby wave, *J. Geophys. Res.*, *107*(D2), 4011, doi:10.1029/2001JD000432.
- Browell, E. V., et al. (1996), Ozone and aerosol distributions and air mass characteristics over the South Atlantic Basin during the burning season, *J. Geophys. Res.*, *101*, 24,043–24,068.
- Cooper, O., et al. (2004), On the life cycle of a stratospheric intrusion and its dispersion into polluted warm conveyor belts, *J. Geophys. Res.*, *109*, D23S09, doi:10.1029/2003JD004006.
- Danielsen, E. F. (1968), Stratospheric-tropospheric exchange based on radioactivity, ozone and potential vorticity, *J. Atmos. Sci.*, *25*, 502–518.
- Denning, R. F., S. L. Guidero, G. S. Parks, and B. L. Gary (1989), Instrument description of the airborne Microwave Temperature Profiler, *J. Geophys. Res.*, *94*, 757–765.
- Dethof, A., A. O’Neill, and J. Slingo (2000), Quantification of the isentropic mass transport across the dynamical tropopause, *J. Geophys. Res.*, *105*, 12,279–12,293.

- Fischer, H., F. G. Wienhold, P. Hoor, O. Bujok, C. Schiller, P. Siegmund, M. Ambaum, H. A. Scheeren, and J. Lelieveld (2000), Tracer correlations in the northern high latitude lowermost stratosphere: Influence of cross-tropopause mass exchange, *Geophys. Res. Lett.*, *27*, 97–100.
- Fishman, J., and W. Seiler (1983), Correlative nature of ozone and carbon monoxide in the troposphere: Implications for the tropospheric ozone budget, *J. Geophys. Res.*, *88*, 3662–3670.
- Hartmann, D. L., K. R. Chan, B. L. Gary, M. R. Schoeberl, P. A. Newman, R. L. Martin, M. Loewenstein, J. R. Podolske, and S. E. Strahan (1989), Potential vorticity and mixing in the South Polar vortex during spring, *J. Geophys. Res.*, *94*, 11,625–11,640.
- Herman, R. L., et al. (1999), Measurements of CO in the upper troposphere and lower stratosphere, *Chemos. Global Change Sci.*, *1*, 83–173.
- Hints, E. J., E. M. Weinstock, J. G. Anderson, R. D. May, and D. F. Hurst (1999), On the accuracy of in situ water vapor measurements in the troposphere and lower stratosphere with the Harvard Lyman- α hygrometer, *J. Geophys. Res.*, *104*, 8183–8189.
- Hoerling, M. P., T. K. Schaack, and A. J. Lenzen (1991), Global objective tropopause analysis, *Mon. Weather Rev.*, *119*, 1816–1831.
- Holton, J. R., P. H. Haynes, M. E. McIntyre, A. R. Douglass, R. B. Hood, and L. Pfister (1995), Stratosphere-troposphere exchange, *Rev. Geophys.*, *33*, 403–439.
- Hoor, P., H. Fischer, L. Lange, J. Lelieveld, and D. Brunner (2002), Seasonal variations of a mixing layer in the lowermost stratosphere as identified by the CO-O₃ correlation from in situ measurements, *J. Geophys. Res.*, *107*(D5), 4044, doi:10.1029/2000JD000289.
- Hoskins, B. J. (1991), Towards a PV- θ view of the general circulation, *Tellus*, *43A*, 27–35.
- Kochanski, A. (1955), Cross sections of the mean zonal flow and temperature along 80°W, *J. Meteorol.*, *12*, 95–106.
- Logan, J. (1999), An analysis of ozonesonde data for the troposphere: Recommendations for testing 3-D models and development of a gridded climatology for tropospheric ozone, *J. Geophys. Res.*, *104*, 16,115–16,150.
- O'Connor, F. M., G. Vaughan, and H. de Backer (1999), Observations of sub-tropical air in the European mid-latitude lower stratosphere, *Q. J. R. Meteorol. Soc.*, *125*, 2965–2986.
- Olsen, M. A., A. R. Douglass, and M. R. Schoeberl (2002), Estimating downward cross-tropopause ozone flux using column ozone and potential vorticity, *J. Geophys. Res.*, *107*(D22), 4636, doi:10.1029/2001JD002041.
- Plumb, R. A., D. W. Waugh, and M. P. Chipperfield (2000), The effects of mixing on tracer relationships in the polar vortices, *J. Geophys. Res.*, *105*, 10,047–10,062.
- Proffitt, M. H., and R. J. McLaughlin (1983), Fast-response dualbeam UV-absorption ozone photometer suitable for use on stratospheric balloons, *Rev. Sci. Instrum.*, *54*, 1719–1728.
- Scott, S. G., T. P. Bui, K. R. Chan, and S. W. Bowen (1990), The meteorological measurement system on the NASA ER-2 aircraft, *J. Atmos. Oceanic Technol.*, *7*, 525–540.
- Shapiro, M. A. (1978), Further evidence of the mesoscale and turbulent structure of upper level jet stream–frontal zone systems, *Mon. Weather Rev.*, *106*, 1100–1110.
- Sprenger, M., and H. Wernli (2003), A Northern Hemispheric climatology of cross-tropopause exchange for the ERA15 time period (1979–1993), *J. Geophys. Res.*, *108*(D12), 8521, doi:10.1029/2002JD002636.
- Stohl, A., et al. (2003), Stratosphere-troposphere exchange: A review, and what we have learned from STACCATO, *J. Geophys. Res.*, *108*(D12), 8516, doi:10.1029/2002JD002490.
- Swinbank, R., and A. O'Neill (1994), A stratosphere-troposphere data assimilation system, *Mon. Weather Rev.*, *122*, 686–702.
- Weinstock, E. M., E. J. Hints, A. E. Dessler, J. F. Oliver, N. L. Hazen, J. N. Demusz, N. T. Allen, L. B. Lapson, and J. G. Anderson (1994), New fast response photofragment fluorescence hygrometer for use on the NASA ER-2 and the Perseus remotely piloted aircraft, *Rev. Sci. Instrum.*, *65*, 3544–3554.
- Wernli, H., and M. Bourqui (2002), A Lagrangian “1-year climatology” of (deep) cross-tropopause exchange in the extratropical Northern Hemisphere, *J. Geophys. Res.*, *107*(D2), 4021, doi:10.1029/2001JD000812.
- World Meteorological Organization (WMO) (1986), Atmospheric ozone 1985, *WMO Global Ozone Res. and Monit. Proj. Rep. 20*, Geneva, Switzerland.
- World Meteorological Organization (WMO) (2003), WMO Scientific Assessment of Ozone Depletion 2002, *WMO Global Ozone Res. Monit. Proj. Rep. 47*, 498 pp, Geneva, Switzerland.
- Zahn, A., et al. (2000), Identification of extratropical two-way troposphere-stratosphere mixing based on CARIBIC measurements of O₃, CO, and ultrafine particles, *J. Geophys. Res.*, *105*, 1527–1535.
- Zahn, A., C. A. M. Brenninkmeijer, and P. F. J. van Velthoven (2004), Passenger aircraft project CARIBIC 1997–2002, Part I: The extratropical chemical tropopause, *Atmos. Chem. Phys. Discuss.*, *4*, 1091–1117.

B. L. Gary and M. J. Mahoney, Jet Propulsion Laboratory, Pasadena, CA 91109-8099, USA.

E. J. Hints, Woods Hole Oceanographic Institution, Woods Hole, MA 02543-1541, USA.

L. L. Pan and W. J. Randel, National Center for Atmospheric Research, 1850 Table Mesa Drive, PO Box 3000, Boulder, CO 80307-3000, USA. (liwen@ucar.edu)